

## Bursts of electron cyclotron emission during disruptions of high beta discharges in the Tokamak Fusion Test Reactor tokamak

A. Janos, K. McGuire, E. Fredrickson, W. Parks, S. Zweben et al.

Citation: *Rev. Sci. Instrum.* **68**, 505 (1997); doi: 10.1063/1.1147617

View online: <http://dx.doi.org/10.1063/1.1147617>

View Table of Contents: <http://rsi.aip.org/resource/1/RSINAK/v68/i1>

Published by the [American Institute of Physics](http://www.aip.org).

---

### Related Articles

Oblique electron-cyclotron-emission radial and phase detector of rotating magnetic islands applied to alignment and modulation of electron-cyclotron-current-drive for neoclassical tearing mode stabilization  
*Rev. Sci. Instrum.* **83**, 103507 (2012)

0.22 THz wideband sheet electron beam traveling wave tube amplifier: Cold test measurements and beam wave interaction analysis  
*Phys. Plasmas* **19**, 093110 (2012)

Measurements of parallel electron velocity distributions using whistler wave absorption  
*Rev. Sci. Instrum.* **83**, 083503 (2012)

HELIOS: A helium line-ratio spectral-monitoring diagnostic used to generate high resolution profiles near the ion cyclotron resonant heating antenna on TEXTOR  
*Rev. Sci. Instrum.* **83**, 10D722 (2012)

Microwave Doppler reflectometer system in LHD  
*Rev. Sci. Instrum.* **83**, 10E322 (2012)

---

### Additional information on *Rev. Sci. Instrum.*

Journal Homepage: <http://rsi.aip.org>

Journal Information: [http://rsi.aip.org/about/about\\_the\\_journal](http://rsi.aip.org/about/about_the_journal)

Top downloads: [http://rsi.aip.org/features/most\\_downloaded](http://rsi.aip.org/features/most_downloaded)

Information for Authors: <http://rsi.aip.org/authors>

## ADVERTISEMENT

### ORTEC MAESTRO<sup>®</sup> V7 MCA Software

For over two decades, MAESTRO has set the standard for Windows-based MCA Emulation. MAESTRO Version 7.0 advances further:

- New!** Windows 7 64-Bit Compatibility with Connections Version 8
- New!** List Mode Data Acquisition for Time Correlated Spectrum Events
- New!** Improved Peak fit calculations
- New!** Improved graphics handling for multiple displays
- New!** Open spectrum files directly from Windows Explorer
- New!** Improved performance with Job Functions and display updates

MAESTRO continues to be the world's most popular nuclear MCA software in a broad range of applications!



**Now 64-bit  
Windows 7  
Compatible!**

[www.ortec-online.com](http://www.ortec-online.com)

# Bursts of electron cyclotron emission during disruptions of high beta discharges in the Tokamak Fusion Test Reactor tokamak

A. Janos, K. McGuire, E. Fredrickson, W. Parks, and S. Zweben  
*Princeton Plasma Physics Laboratory, Princeton, New Jersey 08543*

J. Hastie  
*UKAEA, Culham, Abingdon, Oxon OX14 3DB, United Kingdom*

(Presented on 13 May 1996)

Disruptions are sudden terminations of tokamak plasma discharges. During disruptions at high beta  $\beta \equiv$  plasma pressure/magnetic pressure, short (order of  $\mu$ s) and intense bursts of electron cyclotron emission (ECE), an order magnitude above thermal levels, are observed in the second harmonic electron cyclotron frequency range, which corresponds to 100s of GHz in the Tokamak Fusion Test Reactor tokamak. A unique combination of two, fast, 500 kHz, 20-channel grating polychromator instruments, located at different toroidal positions, is used to measure the emission and characterize these bursts. New insights into the three-dimensional dynamics of these disruptions and the accompanying bursts of ECE have been obtained. Bursts of ECE occur at the beginning of the thermal quenches and exhibit strong toroidal asymmetries. Bursts are localized to the vicinity of the ballooning mode, a fast growing (few ms) medium toroidal mode number ( $n=10-20$ ) precursor, localized toroidally, poloidally, and radially, which triggers the disruptions. Fast-particle losses occur with the explosive growth of the ballooning mode, followed by plasma/wall interaction. Bursts of ECE occur shortly afterwards, within 10s of  $\mu$ s of the fast particle losses. An explanation of the bursting is presented which is consistent both qualitatively and quantitatively, with observations predicting, for example, radiation enhancement factors of  $\approx 10$ . Bursting can be explained not in terms of enhanced excitation of emission but rather in the reduction of absorption of thermal emission. Bursting is consistent with a modification to the electron distribution function  $f_e$  due to a rapid energy or particle exchange between hot electrons and cold electrons from the edge, momentarily reducing the velocity gradient of  $f_c$  in the thermal region. Large edge localized mode events also exhibit bursts of ECE due to a similar sequence of events. © 1997 American Institute of Physics. [S0034-6748(97)72601-7]

## I. INTRODUCTION

Ever since the Tokamak Fusion Test Reactor (TFTR) started producing high  $\beta$  discharges over ten years ago, large bursts of electron cyclotron emission (ECE), higher than thermal levels, were observed. These bursts (Figs. 1 and 2) are most characteristic of these disruptions. However, no explanation could be given which would satisfy all of the observations. We study these since they may offer insight into the dynamics of the disruption process. In particular, the association with the localized nature of the recently identified ballooning mode precursor trigger offered a new and unique opportunity to understand disruption dynamics. Also, numerous astrophysical cases of bursts occur, but are more difficult to understand and are not fully and satisfactorily explained. Finally, an ultimate aim would be to control and/or prevent disruptions. One of the only other times that bursts of ECE are observed in TFTR with comparable robustness is during large edge-localized modes (ELMs) in neutral beam heated H-mode discharges,<sup>1</sup> in which the bursts occur near the edge of the plasma. ECE spikes are excellent indicators of large ELM events in TFTR. An important similarity between effects that ELMs and disruptions have on plasmas was noted in Ref. 2: "both cause a loss of energy and particles on the time scale of the order of 100  $\mu$ s."

## II. INSTRUMENTATION

Two grating polychromator instruments,<sup>3</sup> separated 126° toroidally, measure profiles of second harmonic X-mode ECE along the midplane from the low field side. Frequencies are in the microwave region (150–300 GHz). Each system has 20 channels, a bandwidth of 250 kHz, and is digitized at up to 500 kHz. Plasmas are optically thick, with an optical depth  $\tau \approx 30$ , so that the intensity of the (black body) emission is a measure of the electron temperature  $T_e$  and the MHD, since  $T_e$  can then be assumed to be constant on flux surfaces. Temperature measurements are local as opposed to line-integrated.

## III. SCENARIO OF DISRUPTION FOR HIGH $\beta$ DISCHARGES

Characterization of bursts is best accomplished with an understanding of, and in the context of, the basic scenario of the high  $\beta$  disruption:<sup>3,4</sup> First, a two-dimensional equilibrium becomes unstable to low- $n$  modes. Usually,  $n=1$  internal kink, with  $(m,n)=(1,1)$ , etc. The low- $n$  mode produces a localized high pressure gradient on the outer midplane. This steep gradient destabilizes a linearly fast-growing, ideal, high- $n$  ( $n=10-15$ ) ballooning mode. The ballooning mode is strongly driven in a nonlinear fashion, changing from a multiple-period wave packet to one large prominence (Fig. 1,

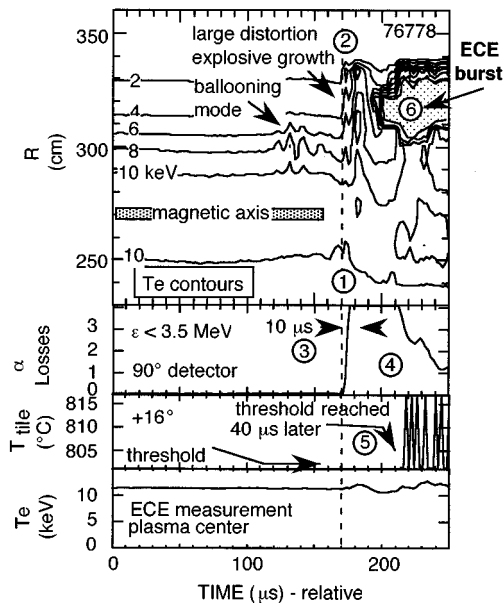


FIG. 1. Timing of explosive growth of precursor, fast particle ( $\alpha$ -particle) losses, wall heating, and ECE bursts in a major disruption.

item 2). Growth of the ballooning mode leads to destabilization of edge modes and island formation. The modes overlap, causing stochasticity in the outer region, from the ballooning mode outward, which develops to encompass the entire cross section,<sup>5</sup> the onset of a thermal quench.

The onset of fast particle  $\alpha$  loss (Fig. 1, items 3 and 4) starts essentially simultaneously with the explosive growth of the ballooning mode (Fig. 1, item 2), and is very abrupt (10  $\mu$ s) (Fig. 1, item 3). While ECE bursts occur during disruptions in deuterium-only discharges as well as deuterium-tritium (D-T) discharges, we use the signal from the fast  $\alpha$  particles as a convenient indicator of particle and

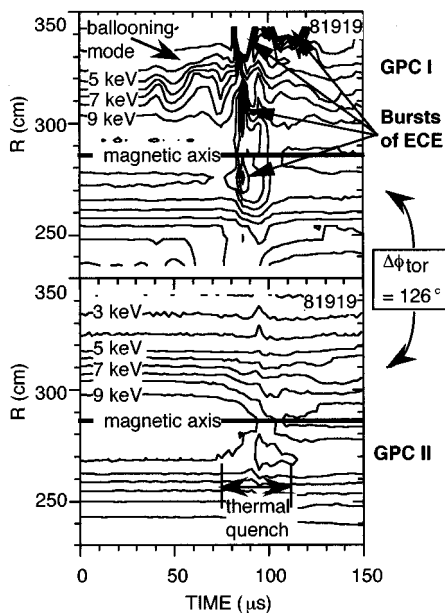


FIG. 2. Comparison of precursor and ECE bursts in a minor disruption. Large toroidal asymmetries in bursts is correlated with location of localized ballooning mode.

energy loss in general. In addition, TFTR has a good system of  $\alpha$  detectors, and these fast  $\alpha$  particles are probably among the first particles lost. The first burst of  $\alpha$  loss (Fig. 1, item 4) which lasts only on the order of 50  $\mu$ s, can be large, releasing 30% of the total fast  $\alpha$  particles lost over the entire disruption event. Within  $\leq 40$   $\mu$ s of the onset of fast particle loss, the inner limiter wall heats to significant levels. Temperatures  $> 800$   $^{\circ}$ C are reached, compared to a few 100  $^{\circ}$ C which is more normal. Wall temperatures are measured by fast, 200 kHz, ir detectors (Fig. 1, item 5). A significant plasma/wall interaction occurs. Near the end of the 40  $\mu$ s, intense ECE bursts are observed near the radius of the ballooning mode (Fig. 1, item 6).

#### IV. CHARACTERIZATION OF BURSTS OF ECE DURING DISRUPTIONS

Key characteristics of ECE bursts follow. They are always observed during thermal quenches of high  $\beta$  disruptions, but not other types of disruptions such as high density or locked mode. They start at the onset of the thermal quench phase and are most intense in the early part of the quench (Figs. 1 and 2), as is determined by comparing bursts from two toroidal locations. The bursts are high intensity, with radiation temperatures from several times to ten times thermal levels. The duration of the bursting ranges from a few  $\mu$ s to the entire duration of the thermal quench (100s  $\mu$ s), and can be composed of a number of spikes of 10–150  $\mu$ s duration. The onset is very fast ( $\mu$ s) and recovery can be just as fast. Sometimes the fast turn-off of bursts is due to cut-off when  $\omega_{pe}^2(\text{edge})$  exceeds  $\omega[\omega - \omega_{ce}(\text{edge})]$ , also indicating strong plasma/wall interaction and a large increase in the edge density. Toroidally, bursts exhibit strong asymmetries (Fig. 2). Bursts are found to be localized in the vicinity of the toroidally, poloidally, and radially localized ballooning mode which triggers the disruption (Fig. 2) thus suggesting that the bursts are closely tied to the ballooning mode evolution and also suggesting that the origin of the bursts is localized. The bursts can remain narrow-band, or quickly can become broad-band, covering a significant fraction of the profile. If there are broad-band bursts, then they either started near the radius of the ballooning mode or are most intense at that radius. The extent of the bursts reflects the extent of the ballooning mode. The bursts of ECE occur after there is plasma/wall interaction.

The localization of the bursts in the vicinity of the ballooning mode explains in part the apparent variability of the bursts identified early in high  $\beta$  research. That is, observation of the burst for a given disruption depends upon whether the ballooning mode was within the field of view of the diagnostic viewing the ECE at the time of disruption. The extent of the ECE bursting is much smaller for minor disruptions compared to major disruptions, in spatial extent, time duration, and intensity. The smaller ECE bursts observed in minor disruptions correlate well with smaller ballooning modes also observed in minor disruptions. In minor disruptions, the smaller extent of the ballooning mode, in space and amplitude, suggests that the reconnection event should be smaller; the fact that the reconnection event is smaller is consistent with the fact that a minor disruption occurs, as opposed to a

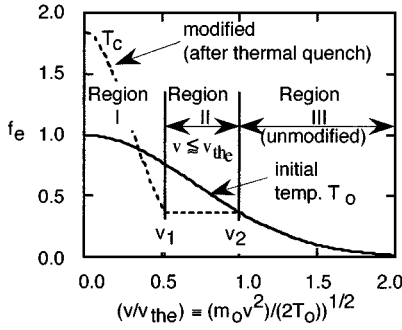


FIG. 3. Model electron distribution function  $f_e(v)$  before and after modification due to thermal quench.

major. Because the ballooning mode is more localized and does not spread as much and as quickly in minor disruptions as opposed to major disruptions, the observed toroidal asymmetries are thus more pronounced.

### V. MODIFICATION OF ELECTRON DISTRIBUTION FUNCTION DUE TO RAPID THERMAL QUENCH

Numerous mechanisms for the generation of the bursts were investigated, including relativistically down-shifted emission from energetic electrons in the plasma core, enhanced emission from anisotropic distortions of the electron distribution function due to magnetohydrodynamic MHD displacements from the kink and ballooning mode,<sup>6</sup> enhanced emission from loss cone distributions due to stochastic fields, and skewed (versus strictly perpendicular) viewing of the emission due to the distortion of the field from ballooning modes. All of these explanations suffered from difficulties agreeing with experimental observations. We present a model which is both qualitatively and quantitatively consistent with the experimental results, and in particular with details of the magnitude, timing, and location of the bursts. The scenario is as follows:

localized MHD mode  $\Rightarrow$  stochastic field formation and fast particle loss  $\Rightarrow$  wall heating and cold electron influx  $\Rightarrow$  electron distribution modification  $\Rightarrow$  bursts of ECE.

We propose that the sudden thermal quench leads to a reduction or flattening of the velocity gradient of the electron distribution function  $f_c$  in the vicinity of thermal velocities  $v_{th}$ . The initial  $f_e$ , a Maxwellian with temperature  $T_0$ , is modified in an isotropic way, conserving particle density (Fig. 3) with a flattened distribution in the region of  $v_{th}$ . This could occur due to a fast exchange of hot or warm electrons with cold electrons from the plasma edge; this would need to occur over a time period shorter than the relaxation time.

The interpretation of ECE measurements is based on the “equation of radiative transfer,” which accounts for both emission and absorption by electrons of different energies occurring at different plasma locations. This equation can be written as

$$\frac{d}{ds} I(\omega, s) = j_n(\omega, s) - a_n(\omega, s) I(\omega, s),$$

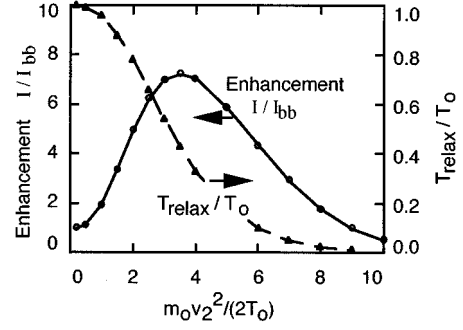


FIG. 4. Calculated enhancement of measured ECE intensity due to modification of  $f_e$  (Fig. 3).

where  $I(\omega, s)$  = intensity,  $j_n(\omega, s)$  = emission coefficient,  $\alpha_n(\omega, s)$  = absorption coefficient, and  $n$  = harmonic number. For radiation through a plasma, incident at point  $a$  and observed at point  $b$ , the solution is

$$I(\omega, b) = I(\omega, a) e^{-\tau_{ab}} + \int_a^b ds j(\omega, s) e^{-\tau_{sb}},$$

where

$$\tau_{sb}(\omega) = \int_s^b ds' a(\omega, s').$$

We solve this for the three regions in Fig. 3 using expressions for the emission and absorption coefficients from Bornatici.<sup>7</sup> These coefficients can be reduced to

$$j_{n=2} = \frac{16\sqrt{2}}{15} \frac{e^2 \omega}{c} \int_0^\infty dt t^{5/2} \delta\left(t - \left(\frac{2\omega_{c_0}}{\omega} - 1\right)\right) f(t)$$

and

$$a_{n=2} = -\left(\frac{8\pi^3 c^2}{\omega^2}\right) \frac{32\sqrt{2}}{15} \frac{e^2 \omega}{c} \frac{1}{2m_0 c^2} \int_0^\infty dt t^{5/2} \times \delta\left[t - \left(\frac{2\omega_{c_0}}{\omega} - 1\right)\right] \frac{\partial}{\partial t} f(t),$$

where  $t \equiv (1/2)(v/c)^2$ . If  $\partial f_e / \partial v$  decreases in Region II (Fig. 4), absorption in that region decreases. These three regions in velocity space, map into three regions in real space. Detected ECE intensity for fixed frequency is the sum of contributions from these regions. We calculate the ratio of the predicted emission relative to initial thermal levels for various initial temperatures  $T_0$  and different modifications to  $f_c$ . The extent of flattening is denoted by  $v_2$  (Fig. 3) and modified Region I temperatures  $T_c$ . The model predicts (Fig. 4) a maximum versus  $v_2$ , with enhancement factors up to  $\approx 7$  for  $T_0 = 5$  keV and  $T_c = 5$  eV, comparable to the experiment for both disruptions and ELMs. Modifications of  $f_c$  in the  $v_{th}$  region are most effective in enhancing emission. Other possible mechanisms investigated predicted enhancements of only  $\leq 10\%$ . Burst do not require the existence of suprathermal electrons, as was previously suggested.<sup>8</sup>

Assuming conservation of energy,  $T_{relax}$  of a final relaxed Maxwellian electron distribution is calculated and shown in Fig. 4. For disruptions where large volumes of plasma are modified,  $T_{relax}/T_0$  agrees well with values observed, i.e., 0.2–0.7.

## VI. DISCUSSION

The similarity in spikes for ELMs is probably due to the similar circumstances: ELMs are synchronized with  $D_\alpha$  spikes, indicating a strong plasma/wall interaction due to the ELM instability. A fast ballooning type instability is thought to be responsible for the ELM events also. The radial location of bursts for ELMs is not very different from that for disruptions, except being slightly further out in radius. In absolute amplitude, bursts for disruptions are larger than those for ELMs.

With this new understanding of the origin of the bursts, they can be used as a new diagnostic to monitor the effects of fast and large plasma/wall interactions which result from the evolution of the magnetic configuration and fast particle and energy transport during high  $\beta$  disruptions and ELMs. There remains the question of whether these bursts would be seen with equal robustness in divertor devices since the plasma/wall interaction scenario could be quite different.

## ACKNOWLEDGMENTS

This work was supported by U.S. DOE Contract No. DE-AC02-76-CH03073 and UKAEA, Culham, England. The authors thank Dr. K. Young and Dr. D. Johnson for supporting the development and operation of these diagnostics.

- <sup>1</sup>A. Janos *et al.*, Proceedings of the IAEA Technical Meeting on H-Mode Physics, 1995 (unpublished).
- <sup>2</sup>Asdex Team, Nucl. Fusion **29**, 1959 (1989).
- <sup>3</sup>A. Janos *et al.*, Rev. Sci. Instrum. **66**, 668 (1995).
- <sup>4</sup>E. Fredrickson *et al.*, *Proceedings of the 15th International Conference on Plasma Physics and Controlled Nuclear Fusion Research* (IAEA, Austria, 1993), IAEA-CN-60/A-2-II-5.
- <sup>5</sup>W. Park, E. D. Fredrickson, A. Janos, J. Manickam, and W. Tang, Phys. Rev. Lett. (to be published).
- <sup>6</sup>R. J. Hastie, Report No. JET-R(94), 03 May 1994 (unpublished).
- <sup>7</sup>M. Bornatici, R. Cano, O. De Barbieri, and R. Engelmann, Nucl. Fusion **23**, 1153 (1983).
- <sup>8</sup>G. Taylor, E. Fredrickson, and A. Janos, Rev. Sci. Instrum. **66**, 830 (1995).